Visualization of the accurate distribution of trace uranium in environmental sample using superconducting technology

Uranium (U) is widely utilized as a fuel for nuclear power generation across the globe. Many countries are planning geological disposal of spent nuclear fuels. The migration behavior of U in subsurface environment is critical for nuclear waste disposal, and a deeper understanding of the interactions between minerals in these subsurface environments and U is essential for assessing the safety of natural barriers involved in its geological disposal [1]. Micro-X-ray fluorescence-X-ray absorption near edge structure (μ-XRF-XANES) analysis is a powerful tool for determining U distribution and chemical species. However, the energy resolution of commonly used semiconductor detectors is insufficient owing to the presence of various elements in environmental samples. Fluorescence X-rays from trace amounts of U can be interfered with by the fluorescence X-rays of other elements (such as Rubidium (Rb)) in the Earth's crust, which complicates the accurate determination of U distribution and chemical species [2].

In this study [3], we utilized a superconducting transition-edge sensor (TES) [4], which offers both high energy resolution and high detection efficiency. The micro-XRF-XANES experiments were conducted at SPring-8 **BL37XU**. The experimental setup is illustrated in Figs. 1(a,b). The XRF spectra of the NIST610 sample were obtained using both a conventional silicon drift detector (SDD) and TES at an excitation energy of 17.2 keV to compare the energy resolutions of the conventional semiconductor detector and TES in the hard X-ray energy region (Fig. 2). Figure 2(a) shows the XRF spectra measured using SDD and TES. The XRF spectrum measured by TES revealed several finer peaks compared to those measured by SDD, indicating that high-energy resolution was maintained from the low- to high-energy regions. Figure 2(b) shows the XRF spectra in the energy range that includes the Rb $K\alpha$ and U $L\alpha_1$ lines, measured using both SDD and TES. In the XRF spectrum obtained with SDD, the Rb $K\alpha$ line at 13.376 keV and the U $L\alpha_1$ line at 13.615 keV were not completely separated, and the XRF peak of the U $L\alpha_1$ line was observed as a structure near the shoulder of the Rb peak in Fig. 2(b). Thus, when using a conventional semiconductor detector, the X-ray fluorescence peaks of Rb and U overlap. By contrast, the XRF spectrum of NIST 610 measured by TES showed that the Rb $K\alpha$ line at 13.376 keV was split into the Rb $K\alpha_1$ line at 13.395 eV and the Rb $K\alpha_2$ line at 13.336 eV. The XRF peak of the U $L\alpha_1$ line at 13.615 keV was fully separated from the Rb $K\alpha_1$ line at 13.395 keV, demonstrating that TES enabled ultrahigh energy resolution analysis.

For the environmental sample, we used biotite collected from the Ningyo Toge U mine in Japan. Figures 3(a,b) show the biotite thin-section sample and a magnified SEM image of the biotite sample, respectively. Mapping analysis was performed on a 75 μm long and 400 μm wide area from the basal of the thin biotite section, indicated by the red square in Fig. 3(b). Figures 3(c,d) compare the mapping analysis results of the biotite sample obtained using SDD and TES. The conventional SDD could only detect the fluorescence X-ray of the Rb $K\alpha$ line (Fig. 3(e)), which is abundant in biotite, and could not accurately detect the signal of trace amounts of U (Fig. 3(c)). Furthermore, TES mapping results revealed that the distribution of Rb and U were different (Fig. 3(d)), as the Rb $K\alpha$ and U $L\alpha_1$ peaks were clearly separated in the XRF spectra obtained using high-energy resolution TES, as shown in Fig. 3(f). These results demonstrate that TES allows for accurate determination of the distribution of trace amounts of U, which is difficult to analyze using conventional semiconductor detectors.

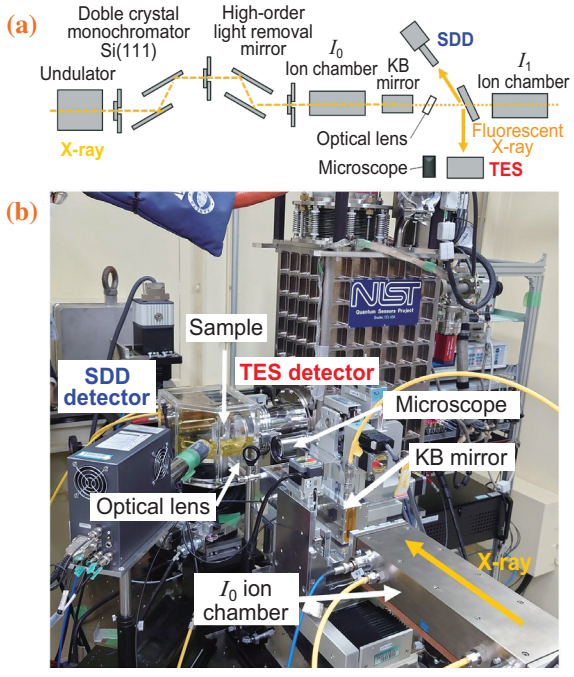

Fig.1. Overview of the experimental setup. **(a)** Schematics illustrate the experimental setup at BL37XU. **(b)** The picture of the setup.

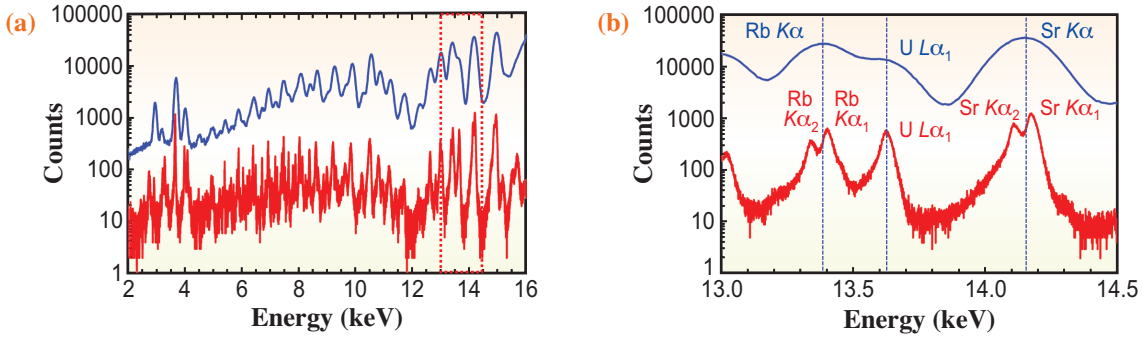

Fig. 2. Comparing energy resolution of SDD and TES in hard X-ray energy region. **(a)** X-ray fluorescence spectra of NIST 610 measured by SDD (blue line) and TES (red line) at an excitation energy of 17.2 keV. **(b)** XRF spectra are indicated by the red dotted line in (a).

Additionally, simultaneous μ-XANES measurements successfully identified the chemical state of U in the biotite, revealing that some of the U was reduced to U(IV). This indicates that U was partially reduced and fixed in biotite, thereby lowering its mobility.

Although this experiment focused on U and Rb in environmental samples, TES has been shown to provide high energy resolution up to the high-energy region of 17 keV. Consequently, TES can be applied to the analysis of other elements with fluorescent X-rays in this energy range up to 17 keV, and its application to various environmental samples is expected in the future.

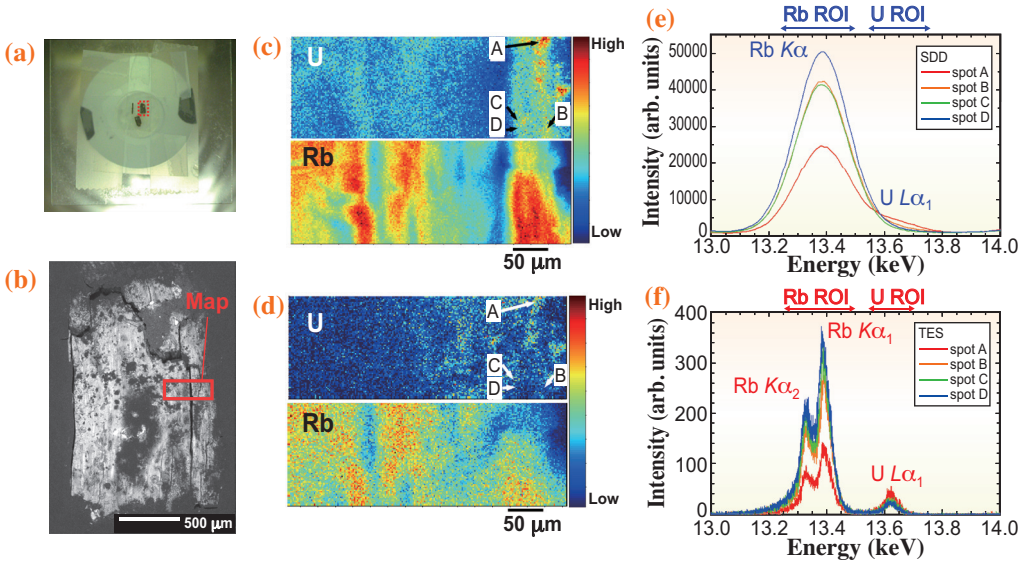

Fig. 3. Micro-X-ray fluorescence imaging of biotite thin sample. **(a)** Optical image of the thin-sectioned sample. **(b)** The magnified SEM image of the red dotted line in (a). The micro-XRF mapping area was shown in a red solid line. Micro-XRF U and Rb map images by **(c)** SDD and **(d)** TES. Micro-XRF spectra of the thin biotite sample measured by **(e)** SDD and **(f)** TES. The region of interest (ROI) of Rb *K*α and U *L*α$_1$ is shown in the upper part of the figures.

Takumi Yomogida[a,b,*], Shinya Yamada[c] and Yoshio Takahashi[b]

[a] Nuclear Science and Engineering Center, Japan Atomic Energy Agency
[b] Department of Earth and Planetary Science, The University of Tokyo
[c] Department of Physics, Rikkyo University

*Email: yomogida.takumi@jaea.go.jp

References

[1] Y. Takahashi *et al.*: Treatise on Geochemistry (Third Edition) **6** (2025) 105.
[2] Y. Yamamoto *et al.*: Appl. Geochem. **23** (2008) 2452.
[3] *T. Yomogida, T. Hashimoto, T. Okumura, S. Yamada, H. Tatsuno, H. Noda, R. Hayakawa, S. Okada, S. Takatori, T. Isobe, T. Hiraki, T. Sato, Y. Toyama, Y. Ichinohe, O. Sekizawa, K. Nitta, Y. Kurihara, S. Fukushima, T. Uruga, Y. Kitatsuji, Y. Takahashi: Analyst. **149** (2024) 2932.*
[4] S. Yamada *et al.*: Rev. Sci. Instrum. **92** (2021) 013103.